# SENSITIVITY TO THE $B_s$–$\overline{B}_s$ MIXING PHASE AT LHCb*

Luis Fernández

On behalf of the LHCb Collaboration

LPHE, Ecole Polytechnique Fédérale de Lausanne, Switzerland

*(Received November 15, 2006)*

We present the sensitivity to the $B_s$–$\overline{B}_s$ mixing phase $\phi_s$ at LHCb, using decays proceeding through $\overline{b} \to \overline{c}c\overline{s}$ quark-level transitions. The performance is assessed by means of toy Monte Carlo simulations, parameterized using the results of full Monte Carlo studies. Both the $\overline{b} \to \overline{c}c\overline{s}$ decays to pure ($B_s \to \eta_c\phi$, $B_s \to D_sD_s$, $B_s \to J/\psi\eta$) and to an admixture of CP eigenstates ($B_s \to J/\psi\phi$) are considered, and used to probe the $B_s$–$\overline{B}_s$ mixing phase through a time-dependent mixing-induced CP measurement.

PACS numbers: 11.30.Er, 12.15.Ff, 12.15.Hh, 13.25.Hw

## 1. Neutral $B_s$–$\overline{B}_s$ system

The description of CP violation in the Standard Model (SM) is based on the CKM picture [1, 2]. The unitary CKM matrix connects the electroweak eigenstates $(d', s', b')$ of the down-type quarks with their mass eigenstates $(d, s, b)$. The complex couplings in the CKM matrix allow CP violation to occur in the quark sector of the SM, provided we have complex physical phases, and at least three generations of quarks.

The unitarity of the quark mixing matrix leads to orthogonality relations that can be represented as triangles in the complex plane. For the $B_s$–$\overline{B}_s$ system, the relevant orthogonality relation is

$$\underbrace{V_{us}V_{ub}^*}_{\mathcal{O}(\lambda^4)} + \underbrace{V_{cs}V_{cb}^*}_{\mathcal{O}(\lambda^2)} + \underbrace{V_{ts}V_{tb}^*}_{\mathcal{O}(\lambda^2)} = 0\,, \tag{1}$$

* Presented at the "Physics at LHC" Conference, Kraków, Poland, July 3–8, 2006.

where relative sizes are indicated using Wolfenstein's parameterization [3]. The corresponding triangle is squashed. The relevant rephasing invariant angle for the study of CP violation is doubly Cabibbo-suppressed:

$$\beta_s \equiv \chi \equiv \arg\left[-\frac{V_{cb}V_{cs}^*}{V_{tb}V_{ts}^*}\right] \approx \lambda^2\eta + \mathcal{O}(\lambda^4) \approx \arg(V_{ts}) - \pi\,. \tag{2}$$

### *1.1. Mixing*

The neutral $B_s$–$\overline{B}_s$ system exhibits particle–antiparticle mixing [4]. In the following, we adopt the phase and sign conventions of [5]. The $B_s$–$\overline{B}_s$ mixing refers to the transitions between the two flavor eigenstates, which are not weak eigenstates, caused by the off-diagonal terms in the effective Hamiltonian describing the particle–antiparticle system. The physical mass eigenstates are defined by $|B_{\rm L,H}\rangle = p|B_s\rangle \pm q|\overline{B}_s\rangle$.

The physical states propagate with well-defined and measurable masses ($M_{\rm H/L}$) and decay widths ($\Gamma_{\rm H/L}$). Their mass difference is $\Delta M_s = M_{\rm H} - M_{\rm L} > 0$, and their total width difference is $\Delta\Gamma_s = \Gamma_{\rm L} - \Gamma_{\rm H}$. The SM predictions for the mixing observables are a non-negligible $\Delta\Gamma_s/\Gamma_s \sim 10^{-1}$ (with $\Gamma_s = (\Gamma_{\rm H} + \Gamma_{\rm L})/2$), and a fast oscillation frequency $\Delta M_s \sim 20\,{\rm ps}^{-1}$.

The particle–antiparticle transitions ($|\Delta F| = 2$) arise within the SM from box diagrams as shown in Fig. 1. The off-diagonal elements of the mass matrix, $M_{12}$, are dominated by internal top-quark exchanges. Since the intermediate states appearing in the determination of $M_{12}$ are virtual, New Physics (NP) could easily contribute to it. On the other hand, the off-diagonal elements of the decay matrix, $\Gamma_{12}$, are dominated by real states to which both $B_s$ and $\overline{B}_s$ may decay. Thus, $\Gamma_{12}$ is almost insensitive to NP.

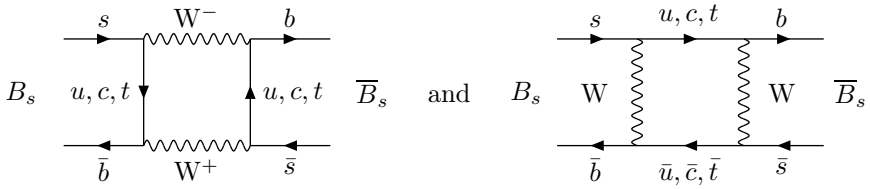



Fig. 1. Leading order box diagrams contributing to the $B_s$–$\overline{B}_s$ mixing in the SM.

The phase difference between $M_{12}$ and $\Gamma_{12}$ represents an observable CP-violating phase. In the SM, it reduces to the $B_s$–$\overline{B}_s$ mixing phase:

$$\phi_s^{\rm SM} = 2\arg[V_{ts}^*V_{tb}] \approx -2\beta_s \sim \mathcal{O}(-0.04)\ {\rm rad}\,. \tag{3}$$

The SM value of $\phi_s$ is very small. Thus, any significant deviation from the SM expectations ($\phi_s = \phi_s^{\rm SM} + \phi_s^{\rm NP}$) would uncover NP.

### *1.2. $\overline{b} \to \overline{c}c\overline{s}$ quark-level transitions*

The study of $B_s$ decays to CP eigenstates proceeding through $\bar{b} \to \bar{c}c\bar{s}$ quark-level transitions enables the determination of the $B_s$–$\overline{B}_s$ mixing phase $\phi_s$. These decays are dominated by the tree-diagram phase, and receive negligible — doubly Cabibbo-suppressed — contributions from penguin diagrams.

There are several decays of interest for the determination of $\phi_s$:

- CP-even eigenstates ($\eta_f = +1$): $B_s \to \eta_c\phi$, $B_s \to D_sD_s$, $B_s \to J/\psi\eta^{(\prime)}$.
- Admixture of CP eigenstates: $B_s \to J/\psi\phi$. The separation of the different states is required, with CP eigenvalues $\eta_f = +1, -1, +1$. The corresponding components will be denoted by $0, \perp, \|$, respectively.

$B_s \to D_sD_s$ being color-allowed, it may be affected by final state interactions. The phase mismatch between the mixing and decay phases allows us to perform a time-dependent mixing-induced CP measurement (see Fig. 2). The relevant complex observable for the description of CP violation in $\bar{b} \to \bar{c}c\bar{s}$ quark-level transitions is:

$$\lambda_f \equiv \frac{q}{p}\frac{\overline{A}_f}{A_f} \approx \eta_f \, e^{-i\phi_s} \,, \tag{4}$$

where we ignored CP violation in the mixing (*i.e.* $q/p = -e^{-i\phi_s}$). We assume the decay amplitudes to be controlled by a single weak phase $\phi_D \equiv \arg[V_{cb}V_{cs}^*] = \mathcal{O}(\lambda^6)$, which is approximatively real (such that the ratio of decay amplitudes is $\overline{A}_f/A_f = -\eta_f \, e^{i2\phi_{\rm D}} \approx -\eta_f$).

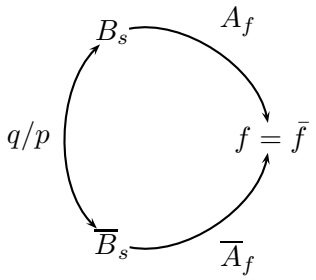



Fig. 2. Mixing-induced CP violation.

The decay rates for initially pure $B_s$ or $\overline{B}_s$ states in $\bar{b} \to \bar{c}c\bar{s}$ or $b \to c\bar{c}s$ quark-level transitions are given by the following expressions for the CP components:

$$R_f\,(t,q)\;\propto\;e^{-\Gamma_s t}\left\{\cosh\frac{\Delta\Gamma_s\,t}{2}-\eta_f\cos\phi_s\,\sinh\frac{\Delta\Gamma_s\,t}{2}\right.$$
$$\left.+\,\eta_f\,q\,D\,\sin\phi_s\,\sin\left(\Delta M_s t\right)\right\}, \qquad (5)$$

where $t$ is the proper time. The result of the flavor tagging (*i.e.* the determination of the initial $b$-meson flavor) is described by $q$, which takes the values of $q=+1$ if the signal meson is tagged as a $B_s$ at production time, $q=-1$ if it is tagged as a $\overline{B}_s$, and $q=0$ if the meson is untagged. The effect of the wrong-tag probability $\omega_{\rm tag}$ is included in the dilution factor $D\equiv(1-2\omega_{\rm tag})$.

We see from (5) that untagged events give access to $\cos\phi_s$ and $\Delta\Gamma_s$. Given that the $\sin\phi_s$ term and the tagging dilution $D$ both modulate the $\Delta M_s$ oscillations, we need to introduce a control sample, *e.g.* $B_s\to D_s\pi$, to help in the determination of $\Delta M_s$ and of $\omega_{\rm tag}$.

### *1.3. $B_s\to J/\psi\phi$ angular analysis*

The $B_s\to J/\psi\phi$ decay requires an angular analysis to separate the different CP eigenstates, which can be done using the linear polarization amplitudes $A_f(t)$. The transversity basis [6] enables to disentangle the CP components in terms of the so-called transversity angle $\theta$. The one-angle angular differential distribution for $B_s\to f$ is:

$$\frac{d\,\Gamma[B_s(t)\to f]}{d\,\cos\theta}\propto\left(|A_0(t)|^2+|A_\parallel(t)|^2\right)\frac{3}{8}\left(1+\cos^2\theta\right)+|A_\perp(t)|^2\,\frac{3}{4}\sin^2\theta\,. \quad (6)$$

The CP components are thus separated by their proper times and angular distributions. Finally, we introduce the observable fraction of CP-odd eigenstates at $t=0$: $R_{\rm T}\equiv|A_\perp|^2/\sum_{f=0,\parallel,\perp}|A_f|^2\sim 20\%$.

### *1.4. $B_s\to D_s\pi$ flavor-specific channel*

$\Delta M_s$ can be extracted from the $B_s\to D_s\pi$ flavor-specific decay channel. Assuming no CP violation in the mixing, the decay rates are:

$$R\,(t,r)\;\propto\;\frac{e^{-\Gamma_s t}}{2}\left\{\cosh\frac{\Delta\Gamma_s t}{2}+r D\cos\left(\Delta M_s t\right)\right\}, \qquad (7)$$

where the results are $r=+1$ for a $B_s$ candidate tagged as unmixed, $r=-1$ for a $B_s$ tagged as mixed, and $r=0$ for an untagged $B_s$ candidate.

## 2. LHCb full Monte Carlo simulation

The LHCb experiment is designed to study rare $b$ decays and CP violation. The high-precision measurements at LHCb will enable to test the CKM picture, and to probe physics beyond the Standard Model. The LHCb detector is a single-arm forward spectrometer, currently in its final construction phase. The main characteristics are the precise vertexing, and good tracking and particle identification.

We assume a $b\bar{b}$ production cross-section of $\sigma_{b\bar{b}} = 500\,\mu$b at the LHC. LHCb will run at a nominal luminosity of $\mathcal{L} = 2\times10^{32}\,\mathrm{cm}^{-2}\mathrm{s}^{-1}$, corresponding to an annual (*i.e.* $10^7$ s) integrated luminosity of $2\,\mathrm{fb}^{-1}$. The trigger system is designed to reduce the event rate to $\sim 2\,$kHz.

The design and performance of the detector have been optimized using a realistic full Monte Carlo simulation. The $pp$ collisions at $\sqrt{s} = 14\,$TeV are generated, including pileup. Particles are tracked through the detector setup, accounting for the detector's response, material, and spill-over effects. After the trigger, the events are reconstructed off-line and signal events are identified by means of selection and flavor tagging algorithms.

The following is a summary of the $\phi_s$ studies described in [7].

### *2.1. Full Monte Carlo results*

The results from full MC studies are used to parameterize the fast simulation and assess the sensitivities to $\phi_s$, using the following channels:

- $B_s \to J/\psi(\mu^+\mu^-)\phi(K^+K^-)$;
- $B_s \to \eta_c(\pi^+\pi^-\pi^+\pi^-, \pi^+\pi^-K^+K^-, K^+K^-K^+K^-)\phi(K^+K^-)$;
- $B_s \to J/\psi(\mu^+\mu^-)\eta(\gamma\gamma, \pi^+\pi^-\pi^0)$;
- $B_s \to D_s^+(K^+K^-\pi^+)D_s^-(K^+K^-\pi^-)$.

The $B_s \to D_s^-(K^+K^-\pi^-)\pi^+$ decay is used as control channel.

The results from the full simulation are summarized in Table I. The yields correspond to the expected number of triggered and untagged off-line selected events with an integrated luminosity of $2\,\mathrm{fb}^{-1}$. The background-to-signal ratio $B/S$ is determined using mainly inclusive $b\bar{b}$ events. The mean of the per-event proper time errors is denoted by $\langle\tau_{\mathrm{fit}}^{\mathrm{err}}\rangle$, and the proper time scale factor by $\Sigma_\tau$ (width of pull). Finally, $\varepsilon_{\mathrm{tag}}$ denotes the tagging efficiency and $\omega_{\mathrm{tag}}$ the wrong tag fraction.

The proper time and its error are extracted on an event-by-event basis using a least-squares fit. The distributions of the proper time errors $\tau_{\mathrm{fit}}^{\mathrm{err}}$ (scaled with $\Sigma_\tau$) are shown in Fig. 3. Most channels have a proper time resolution below 40 fs, precise enough to resolve the fast $B_s$–$\overline{B}_s$ oscillations.

TABLE I

Inputs from the full MC simulation used for the fast simulations.

| Parameters | $J/\psi\phi$ | $\eta_c\phi$ | $D_sD_s$ | $J/\psi\eta(\gamma\gamma)$ | $J/\psi\eta(\pi\pi\pi)$ | $D_s\pi$ |
|---|---|---|---|---|---|---|
| $2\,\text{fb}^{-1}$ yield [k] | 131 | 3 | 4 | 8 | 3 | 120 |
| $B/S$ | 0.12 | 0.6 | 0.3 | 2.0 | 3.0 | 0.4 |
| $\sigma_{B_s}$ [MeV/$c^2$] | 14 | 12 | 6 | 34 | 20 | 14 |
| $\langle\tau_{\text{fit}}^{\text{err}}\rangle$ [fs] | 29.5 | 26.2 | 44.4 | 30.4 | 25.5 | 32.9 |
| $\Sigma_\tau$ | 1.22 | 1.16 | 1.26 | 1.22 | 1.32 | 1.21 |
| $\omega_{\text{tag}}$ [%] | 33 | 31 | 34 | 35 | 30 | 31 |
| $\varepsilon_{\text{tag}}$ [%] | 57 | 66 | 57 | 63 | 62 | 63 |

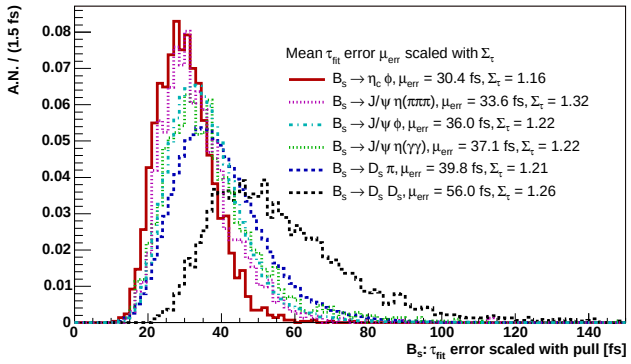



Fig. 3. Distribution of the proper time errors [fs] (scaled with $\Sigma_\tau$) for the different $B_s$ channels, as obtained from the full MC. The normalization is arbitrary.

## 3. Sensitivity to the $B_s$–$\overline{B}_s$ mixing phase at LHCb

The sensitivities to the $B_s$–$\overline{B}_s$ mixing parameters are determined by means of fast parameterized simulations, with the results of Table I as inputs. We generate $\sim$ 225 experiments with the nominal set of SM parameters $M_{B_s} = 5369.6\,\text{MeV}/c^2$, $\Delta M_s = 17.5\,\text{ps}^{-1}$, $\phi_s = -0.04\,\text{rad}$, $\Delta\Gamma_s/\Gamma_s = 0.15$, $\tau_s = 1/\Gamma_s = 1.45\,\text{ps}$, and $R_{\text{T}} = 0.2$ (for $B_s \to J/\psi\phi$).

### *3.1. Fast Monte Carlo*

The different parameters are extracted by performing a likelihood fit to the mass, proper time, and transversity angle (for $B_s \to J/\psi\phi$) distributions, including a background contribution. The $\bar{b} \to \bar{c}c\bar{s}$ likelihood is simultaneously maximized with a similar likelihood for the $B_s \to D_s\pi$ control sample. We use the following models:

**Mass:** a Gaussian (signal) and an exponential (background) are used (see Fig. 4), which determine the signal and background probabilities.

**Transversity angle:** for the $B_s \to J/\psi\phi$ sample the distribution (6) is used, assuming a flat background (see Fig. 5).

**Proper time:** the signal decay rates are taken from (5) for the $\bar{b} \to \bar{c}c\bar{s}$ sample, from (7) for $B_s \to D_s\pi$, and exponentials are used for the background. The rates are weighted by an acceptance function. The signal proper time resolution function depends on $\tau_{\rm fit}^{\rm err}$ scaled with $\Sigma_\tau$. We illustrate in Fig. 6 the rates for CP-even eigenstates, and in Fig. 7 the contributions to the proper time for the $B_s \to J/\psi\phi$ sample.

The background properties are determined from the $B_s$ mass sidebands. The physics parameters, extracted in the signal region with all other parameters fixed, are $\phi_s$, $\Delta M_s$, $\Delta\Gamma_s/\Gamma_s$, $\tau_s = 1/\Gamma_s$, $\omega_{\rm tag}$, and $R_{\rm T}$ (for $B_s \to J/\psi\phi$). The sensitivity to a parameter corresponds to the r.m.s. of the distribution of the fit outputs.

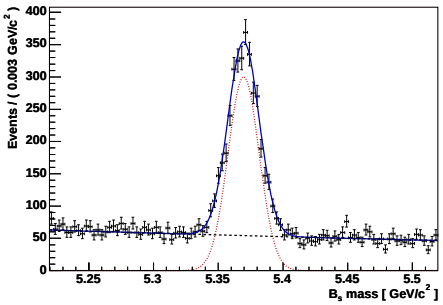



Fig. 4. Likelihood projection onto the mass [GeV/$c^2$] for $B_s \to \eta_c\phi$. Solid: all contributions. Dotted: signal. Dashed: background.

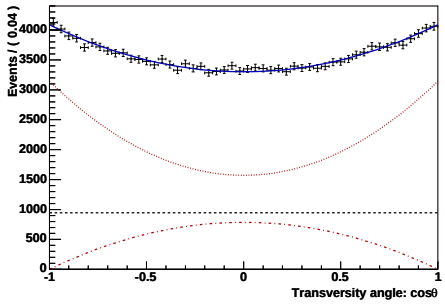



Fig. 5. Likelihood projection onto $\cos\theta$ for $B_s \to J/\psi\phi$ in the total mass window. Solid: all contributions. Dotted: CP-even. Dashed-dotted: CP-odd. Dashed: background.

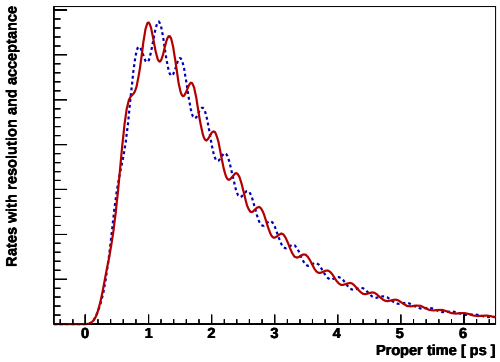



Fig. 6. Signal decay rates [ps] of $\bar{b} \to \bar{c}c\bar{s}$ transitions to CP-even eigenstates, with a 30% wrong-tag fraction, a 35 fs proper-time resolution, and $\phi_s = -0.2$ rad. Solid: tagged $B_s$. Dashed: tagged $\overline{B}_s$.

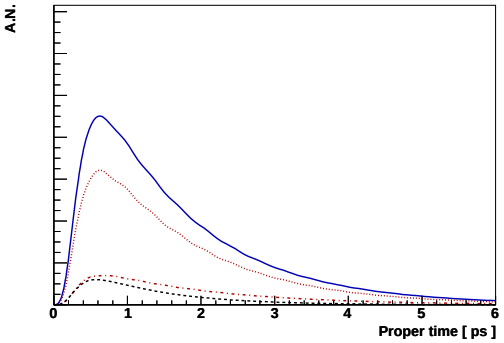



Fig. 7. Likelihood projection onto the proper time [ps] in the signal region, for $B_s \to J/\psi\phi$ events initially tagged as $B_s$. Solid: all contributions. Dotted: CP-even. Dashed-dotted: CP-odd. Dashed: background.

### *3.2. Fit results*

The sensitivities to $\phi_s$ from the simultaneous fits are given in Table II. The best performance is from $B_s \to J/\psi\phi$, although we performed an angular analysis. The contribution from pure CP-eigenstates is small, but non-negligible. For $10\,\text{fb}^{-1}$, we get a statistical uncertainty $\sigma(\phi_s) = \pm 0.0098$ rad.

The sensitivity to $\phi_s$ gently decreases with $|\phi_s|$, and does not depend much on $\phi_s$. For instance, the significance is of $\sim 7\sigma$ for $\phi_s = -0.2$ rad from $B_s \to J/\psi\phi$ alone, with $2\,\text{fb}^{-1}$. In addition LHCb will have access to $\Delta M_s$ with a small statistical uncertainty $\sigma(\Delta M_s) = \pm 0.007\ \text{ps}^{-1}$ (from $B_s \to D_s\pi$, for $\Delta M_s = 17.5\,\text{ps}^{-1}$, and with $2\,\text{fb}^{-1}$).

TABLE II

Combined expected statistical errors on a SM $\phi_s$ with $2\,\text{fb}^{-1}$.

| Channels | $\sigma(\phi_s)$ [rad] | weight $(\sigma/\sigma_i)^2$ [%] |
|---|---|---|
| $B_s \to J/\psi\eta(\pi^+\pi^-\pi^0)$ | 0.142 | 2.3 |
| $B_s \to D_s D_s$ | 0.133 | 2.6 |
| $B_s \to J/\psi\eta(\gamma\gamma)$ | 0.109 | 3.9 |
| $B_s \to \eta_c\phi$ | 0.108 | 3.9 |
| Pure CP eigenstates | **0.060** | **12.7** |
| $B_s \to J/\psi\phi$ | 0.023 | 87.3 |
| All CP eigenstates | **0.022** | **100.0** |

## 4. Conclusions

We presented a method to extract the $B_s$–$\overline{B}_s$ mixing phase at LHCb, using $\bar{b} \to \bar{c}c\bar{s}$ quark-level transitions. The combined statistical sensitivity obtained is $\sigma(\phi_s) = \pm 0.022\,\text{rad}$, corresponding to a $\sim 2\sigma$ measurement for a Standard Model $\phi_s = -0.04\,\text{rad}$, and with $2\,\text{fb}^{-1}$. The sensitivity is dominated by $B_s \to J/\psi\phi$, with however a substantial $\sim 13\%$ contribution from decays to pure CP-eigenstates ($B_s \to \eta_c\phi$, $B_s \to D_s D_s$, $B_s \to J/\psi\eta$). It will allow LHCb to detect sizable New Physics effects.

In conclusion, LHCb has the potential to perform the first measurement of $\phi_s$, to test the consistency with the Standard Model expectations, and to possibly uncover New Physics that may be hiding in the $B_s$–$\overline{B}_s$ mixing.

The author would like to thank Olivier Schneider for his careful reading of this writeup, and for his useful comments.

## REFERENCES

[1] N. Cabibbo. *Phys. Rev. Lett.* **10**, 531 (1963).
[2] M. Kobayashi, T. Maskawa. *Prog. Theor. Phys.* **49**, 652 (1973).
[3] L. Wolfenstein. *Phys. Rev. Lett.* **51**, 1945 (1983).
[4] G.C. Branco, L. Lavoura, J.P. Silva. *CP Violation*, Oxford U.P., 1999.
[5] I. Dunietz, R. Fleischer, U. Nierste. *Phys. Rev.* **D63**, 114015 (2001).
[6] A.S. Dighe *et al.*, *Phys. Lett.*, **B369**, 144 (1996).
[7] L. Fernández. EPFL Ph.D. Thesis 3613, CERN-THESIS/2006-042, 2006.